Auditory brainstem and middle latency responses recorded at fast rates with randomized stimulation

Joaquin T. Valderrama,[a] Angel de la Torre, Isaac M. Alvarez, and Jose C. Segura
Department of Signal Theory, Telematics and Communications, CITIC-UGR, University of Granada, Granada 18071, Spain

A. Roger D. Thornton
MRC Institute of Hearing Research, Royal South Hants Hospital, Southampton SO14 OYG, United Kingdom

Manuel Sainz[b] and Jose L. Vargas
San Cecilio University Hospital, ENT Service, Granada 18012, Spain

(Received 21 March 2014; revised 14 October 2014; accepted 20 October 2014)

Randomized stimulation and averaging (RSA) allows auditory evoked potentials (AEPs) to be recorded at high stimulation rates. This method does not perform deconvolution and must therefore deal with interference derived from overlapping transient evoked responses. This paper analyzes the effects of this interference on auditory brainstem responses (ABRs) and middle latency responses (MLRs) recorded at rates of up to 300 and 125 Hz, respectively, with randomized stimulation sequences of a jitter both greater and shorter than the dominant period of the ABR/MLR components. Additionally, this paper presents an advanced approach for RSA [iterative-randomized stimulation and averaging (I-RSA)], which includes the removal of the interference associated with overlapping responses through an iterative process in the time domain. Experimental results show that (a) RSA can be efficiently used in the recording of AEPs when the jitter of the stimulation sequence is greater than the dominant period of the AEP components, and (b) I-RSA maintains all the advantages of RSA and is not constrained by the restriction of a minimum jitter. The significance of the results of this study is discussed. © *2014 Acoustical Society of America*.
[http://dx.doi.org/10.1121/1.4900832]

PACS number(s): 43.66.Yw, 43.64.Ri, 43.64.Yp [ELP] Pages: 3233–3248

I. INTRODUCTION

Auditory evoked potentials (AEPs) are a set of low-amplitude voltage peaks (usually less than 1 μV at the electrodes), generated in different parts of the auditory pathway in response to a stimulus. AEPs can be classified according to their generator site and their peak latency (time between the stimulus onset and the occurrence of the peaks), which ranges between 1 ms and 0.5 s. The recording of AEPs is extensively used in both human and animal studies because of its noninvasive nature. The auditory brainstem response (ABR) is a particular AEP partly generated in the cochlea, in the auditory nerve and in the brainstem (Eggermont, 2007; Pratt, 2011). The ABR comprises a number of waves that occur within the first 10 ms from stimulus onset. These waves are identified by sequential Roman numerals, as originally proposed by Jewett and Williston (1971). Although up to seven waves can be identified in the ABR, the most robust peaks are waves I, III, and V. The recording of ABR signals is commonly used in hospital and clinics worldwide as a hearing screening tool, to detect the hearing threshold, and to detect hearing impairments such as vestibular schwannomas and Ménière's disease (Kacker and Deka, 1986; Podoshin *et al.*, 1986; Hall, 2007; Bush *et al.*, 2008). The middle latency response (MLR) is generated in the auditory thalamocortical system. The MLR has latencies from 10 to 60 ms, and comprises the components N_a, P_a, N_b, and P_b (Eggermont, 2007; Pratt, 2011). The longer latency component of the MLR is usually affected by attention and is difficult to record under sleep and sedation, limiting the clinical utility of these signals to the assessment of cooperative children and adults (Pratt, 2007). MLR signals are typically used in clinical practice to evaluate the central auditory nervous system and in the assessment of auditory-pathway integrity in cochlear implant candidates, since electrically elicited MLR signals are less contaminated by the stimulus artifact than electrical ABR signals (Fifer and Sierra-Irizarry, 1988; Hall, 2007; Pratt, 2007, 2011).

AEPs are conventionally elicited by stimuli presented periodically (Wong and Bickford, 1980; Elberling and Don, 2007), i.e., with a constant inter-stimulus interval (ISI). This method has the limitation that the ISI must be greater than the averaging window to avoid contamination of the recording by the adjacent responses; otherwise it would not be mathematically possible to recover the overlapping AEP (Zollner *et al.*, 1976; Kjaer, 1980; Jewett *et al.*, 2004). Considering standard averaging windows of 10 ms for ABR signals and 100 ms for MLR signals, ABRs and MLRs cannot be recorded with the conventional method at rates higher than 100 and 10 Hz, respectively. However, the recording of AEPs at higher rates presents certain advantages, as several authors have reported. First, the recording of AEPs at high rates allows the study of neural adaptation (Lasky, 1997; Burkard *et al.*, 1990; Valderrama *et al.*, 2014a). Other

[a]Author to whom correspondence should be addressed. Electronic mail: jvalderrama@ugr.es
[b]Also at: Department of Surgery and its Specialties, University of Granada, Granada 18012, Spain.

authors state that high stimulation rates may improve accuracy in estimating the hearing threshold of a subject (Leung *et al.*, 1998). High stimulation rates have also been used to detect certain pathologies (e.g., Don *et al.*, 1977; Stockard *et al.*, 1978; Yagi and Kaga, 1979; Jiang *et al.*, 2000; Thornton *et al.*, 2006; Bohorquez *et al.*, 2009). Additionally, some authors have concluded that the use of high stimulation rates may speed up hearing screening, since less recording time would be necessary in order for a specific number of averaged auditory responses (sweeps) to be obtained (Thornton and Slaven, 1993; Leung *et al.*, 1998; Bell *et al.*, 2001, 2002). However, neural adaptation produces changes in the morphology of the responses, decreasing the signal-to-noise ratio (SNR) of the response. Whether or not high rates are useful in the recording of AEPs in less time is currently controversial (Burkard and Don, 2007).

Various methods have emerged to overcome the rate limitation imposed by the conventional technique. These methods use jittered stimulation sequences with specific properties in the time and frequency domains that allow the recovery of overlapping transient evoked responses. The *jitter* of a stimulation sequence measures the dispersion of the ISI compared with a periodical presentation of stimuli, with constant ISI. The most relevant methods used to obtain AEPs at high rates are maximum length sequences (MLS) (Eysholdt and Schreiner, 1982), ADJAR (Woldorff, 1993), quasiperiodic sequence deconvolution (QSD) (Jewett *et al.*, 2004), continuous loop averaging deconvolution (CLAD) (Ozdamar *et al.*, 2003a; Ozdamar *et al.*, 2003b; Delgado and Ozdamar, 2004; Ozdamar and Bohorquez, 2006), least-squares (LS) deconvolution (Bardy *et al.*, 2014a), and randomized stimulation and averaging (RSA) (Valderrama *et al.*, 2012).

The MLS, ADJAR, QSD, CLAD, and LS methods obtain the AEP by a deconvolution procedure. The fundamentals of deconvolution of overlapping responses are described below. The recorded electroencephalogram (EEG) $y(t)$ can be represented as the convolution of a stimulation signal $s(t)$ and an AEP $h(t)$ plus noise $n(t)$: $y(t) = s(t) * h(t) + n(t)$. In the frequency domain, this equation would yield $Y(f) = S(f) \cdot H(f) + N(f)$. The AEP in the frequency domain $H(f)$ can be worked out as $H(f) = Y(f)/S(f) - N(f)/S(f)$. In this equation, the value of $N(f)$ is unknown. Therefore, the AEP in the frequency domain can be estimated as $\widehat{H}(f) = Y(f)/S(f)$, considering $N(f)/S(f)$ as the error between the estimated and the real AEP. Accurate estimation of $\widehat{H}(f)$ requires (a) the reduction of the power of the noise distribution $N(f)$ by averaging, and (b) the selection of a stimulation sequence $s(t)$ whose frequency components $S(f)$ are not close to zero, otherwise the noise at that frequency would be amplified, leading to instability. Finally, estimation of the AEP in the time domain is the inverse Fourier transform (IFFT) of $\widehat{H}(f)$: $\widehat{h}(t) = \mathrm{IFFT}\{\widehat{H}(f)\}$ (Jewett *et al.*, 2004; Ozdamar and Bohorquez, 2006; Valderrama *et al.*, 2014a).

The MLS method has been widely used not only with AEPs (e.g., Leung *et al.*, 1998; Bohorquez and Ozdamar, 2006; Lavoie *et al.*, 2010), but also with transient evoked otoacoustic emissions (e.g., Hine *et al.*, 2001; Thornton and Slaven, 1993; de Boer *et al.*, 2007). The distribution of the ISI in this method is adjusted to De-Bruijn sequences, in which a k-ary de-Bruijn sequence $B(k, n)$ of order n of a given alphabet A is a pseudorandom cyclic sequence with size k for which every possible subsequence of length n appears in the sequence exactly once (Tuliani, 2001; Burkard *et al.*, 1990). The nature of De-Bruijn sequences imposes on MLS the restriction of a very high jitter (Jewett *et al.*, 2004; Ozdamar *et al.*, 2007). Some authors believe that high-jittered stimulation sequences are a disadvantage in recording AEPs, because the morphology of the response associated with a stimulus not only depends on the averaged stimulation rate, but also on the preceding ISI; therefore, high-jittered stimulation sequences could evoke auditory responses of different morphology (especially at high rates), and the assumption of a time-invariant response would not be accomplished (Jewett *et al.*, 2004; Ozdamar and Bohorquez, 2006; Valderrama *et al.*, 2014a). The ADJAR technique obtains the transient AEP iteratively in the time domain by convolving the AEP estimate in each iteration with the statistical ISI distribution of the stimulation sequence to estimate the separate effects of preceding and succeeding stimuli on the averaged response. This technique has been widely used in event-related potentials (ERPs) (Bekker *et al.*, 2005; Wang *et al.*, 2008), however, this method has been found difficult to implement (Talsma and Woldorff, 2005; Wang *et al.*, 2006) and problems of instability have been reported by some authors (Bardy *et al.*, 2014a). The QSD, CLAD, and LS methods present different approaches to deconvolve overlapping auditory responses evoked by low-jittered stimuli. These methods have been efficiently used in several clinical and research applications (e.g., Bohorquez *et al.*, 2009; Gutschalk *et al.*, 2009; Presacco *et al.*, 2010; Wang *et al.*, 2013; Bardy *et al.*, 2014b).

In contrast to the MLS, ADJAR, QSD, CLAD, and LS methods, RSA does not perform deconvolution. The approach taken by the RSA method consists of averaging a number of sweeps, corresponding to a burst of stimuli in which the ISI varies randomly according to a predefined probability distribution (randomized stimulation). The RSA method includes a digital blanking process, which considers null values in the average process any samples of the EEG contaminated by stimulus artifact. The main advantages of the RSA method are that (a) it facilitates precise control of the jitter of the stimulation sequence, (b) randomized stimulation sequences are easy to generate, since they are not subject to restrictions in the frequency domain, because RSA does not perform deconvolution, and (c) it allows sweeps to be processed separately. These particular advantages were used in Valderrama *et al.* (2014a) to carry out a study of the fast and slow mechanisms of neural adaptation in humans through the *separated responses* method, which is based on the categorization of sweeps according to their preceding ISI. The categorization of responses according to their preceding ISI may be accomplished because of the individual processing of sweeps that is allowed by RSA. Additionally, the separate processing of responses allows artifact-rejection techniques to be used more efficiently. In RSA, each sweep can be individually accepted or rejected for averaging. In contrast, deconvolution-based methods process blocks of responses, resulting in a less flexible application of the artifact rejection procedure, since the portions rejected for

averaging in these methods are greater than in RSA. The RSA method does, however, have some limitations. Since RSA does not perform deconvolution, this method must deal with interference derived from the contamination produced by overlapping adjacent responses. Interference associated with overlapping responses can be reduced with averaging in RSA provided that the amount of jitter is large enough to enable positive and negative components of such interference to be canceled with averaging (Valderrama *et al.*, 2012). In addition to this, the digital blanking process in RSA entails non-uniform averaging of auditory responses along the averaging window, and small amounts of jitter could lead to significant differences in terms of quality between different segments of the response. For these reasons, the RSA method requires stimulation sequences with a minimum amount of jitter.

In this paper we analyze the performance of the RSA method in different jittering conditions, and we present a new approach for RSA that includes the estimation and suppression of the interference associated with overlapping adjacent responses through an iterative process in the time domain. We have called this evolution of RSA "iterative-randomized stimulation and averaging" (I-RSA). This new approach maintains the advantages of RSA while eliminating the need for a digital blanking process, and thus also eliminating the limitation of the minimum amount of jitter that is imposed in RSA. In this paper, we analyze the interference associated with overlapping responses in the RSA and I-RSA methods with both real and artificially synthesized ABR and MLR signals obtained at different stimulation rates with both long and short jitter distributions. Portions of this research were presented at the International Evoked Response Audiometry Study Group 2013 meeting held in New Orleans, LA (Valderrama *et al.*, 2013).

II. METHODS

A. RSA

The RSA method consists of averaging auditory responses, corresponding to a burst of stimuli in which the ISI varies randomly according to a predefined probability distribution (randomized stimulation). The RSA technique involves a digital blanking process to minimize the effect of the stimulus artifact in overlapping responses. The digital blanking process considers as null values any EEG samples in which stimulus artifact occurs. Using RSA notation (Valderrama *et al.*, 2012), let $y(n)$, $s(n)$ $(n=1,\ldots,N)$, J, and N be, respectively, the digitized EEG, the synchronization signal (indicating with the value of 1 the start of each stimulus, and 0 otherwise), the length of the averaging window, and the total number of EEG samples. Considering a stimulation sequence with K stimuli, the index of the samples in which each stimulus starts can be represented by $m(k)$ $(k=1,\ldots,K)$. Hence, $s(m(k))=1\ \forall k$. The blanking signal differentiates valid samples of the EEG (value 1) from samples contaminated by the stimulus artifact (value 0). The duration of blanking depends on the duration of stimulus artifact. The implementation of blanking of 1 ms duration is appropriate for short duration stimuli, e.g., clicks. In this case, the blanking signal $b(n)$ $(n=1,\ldots,N)$ considers as null values 0.2 ms before and 0.8 ms after each stimulus

$$b(n)=\begin{cases}0 & \text{if } n\in[m(k)-0.2\text{ms}\cdot f_s, m(k)+0.8\text{ms}\cdot f_s]\forall k\\ 1 & \text{otherwise,}\end{cases} \tag{1}$$

considering f_s the sampling frequency. Longer-duration stimulus artifacts would require a longer-duration blanking signal. The AEP $\hat{x}(j)$ $(j=1,\ldots,J)$ is estimated in RSA by averaging the sections of the digitized EEG not contaminated by the stimulus artifact

$$\hat{x}(j)=\frac{\sum_{k=1}^{K} b\big(m(k)+j\big)\cdot y\big(m(k)+j\big)}{\sum_{k=1}^{K} b\big(m(k)+j\big)}. \tag{2}$$

The RSA method is fully described in Valderrama *et al.* (2012). In comparison with other methods based on deconvolution, RSA (a) allows a precise control of the jitter of the stimulation sequence, (b) presents generation of stimulation sequences that is not subject to any particular constraint in the frequency domain, and (c) allows auditory responses to be processed separately. However, since RSA does not perform deconvolution, this method must deal with interference associated with overlapping adjacent responses, and the amount of jitter of the stimulation sequences in RSA must therefore be greater than the dominant period of the AEP components in order for positive and negative components of this interference to be canceled with averaging. The dominant period of an AEP can be estimated through the autocorrelation function as the shift at which the closest maximum correlation occurs (Oppenheim and Schafer, 1999). Figure 1 shows the autocorrelation function for given high-quality ABR and MLR signals. This figure shows that the dominant period of ABR and MLR signals is about 2 and 25 ms, respectively, which is consistent with previous studies (Rudell, 1987; Delgado and Ozdamar, 1994; Galambos *et al.*, 1981; Picton *et al.*, 1992; Pastor *et al.*, 2002; Pratt, 2007).

Moreover, the digital blanking process included in RSA causes non-uniform averaging along the averaging window, i.e., the number of averaged samples along the averaging window varies according to the amount of jitter of the stimulation sequence and the duration of digital blanking. Averaging a number of auditory responses below a predefined threshold of the available samples could produce noticeable differences in terms of quality between different segments of the response. The quality loss associated to digital blanking can be estimated according to the following procedure. Let σ_s and σ_n be the standard deviation for the AEP and noise, respectively, in the recorded signal, and $\hat{\sigma}_s$ and $\hat{\sigma}_n$ the corresponding standard deviations after averaging. If N sweeps are involved in the averaging: $\hat{\sigma}_n=\sigma_n/\sqrt{N}$, while $\hat{\sigma}_s=\sigma_s$. Therefore, the SNR of the averaged response is

$$\begin{aligned}\text{SNR}_{\hat{x}_N}(\text{dB}) &= 20\cdot\log_{10}\left(\frac{\hat{\sigma}_s}{\hat{\sigma}_n}\right)=20\cdot\log_{10}\left(\frac{\sigma_s}{\sigma_n}\cdot\sqrt{N}\right)\\ &= \text{SNR}_x(\text{dB})+10\cdot\log_{10}(N),\end{aligned} \tag{3}$$

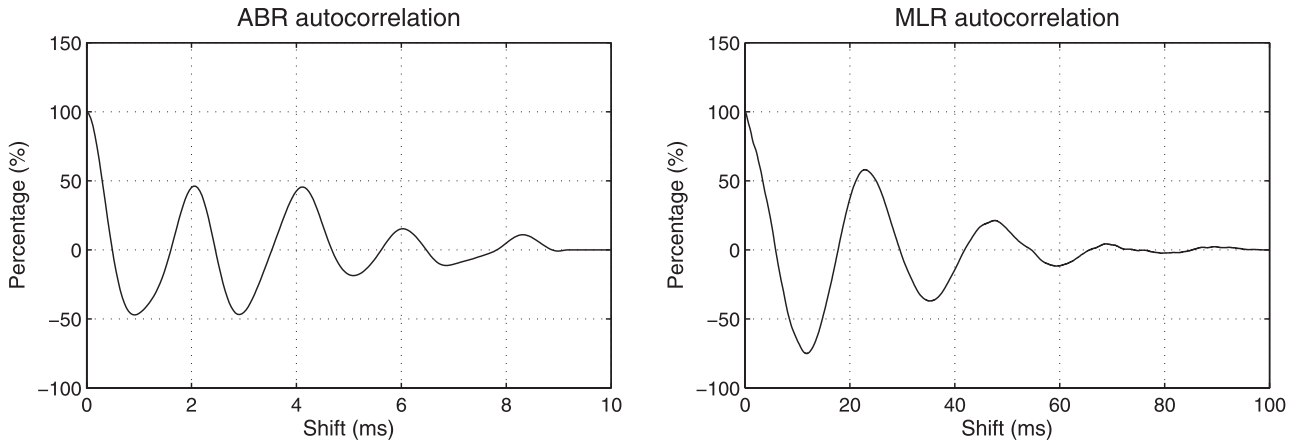

FIG. 1. Autocorrelation function for given high-quality ABR and MLR signals. This figure shows that the dominant period of ABR and MLR signals is about 2 and 25 ms, respectively.

where SNR_x is the SNR of the raw EEG. If a fraction P of the sweeps are available for a sample affected by the blanking procedure, $N \cdot P$ sweeps are averaged instead of N and the SNR will be affected,

$$SNR_{\hat{x}_{N\cdot P}}(\text{dB}) = SNR_{\hat{x}_N}(\text{dB}) + 10 \cdot \log_{10}(P). \quad (4)$$

This points out that averaging at least 70% of the available samples would produce a maximum quality loss between different segments of the response of 1.55 dB. Other averaging thresholds, e.g., 50%, 25%, or 10% would produce maximum quality losses of, respectively, 3, 6, and 10 dB.

Figure 2 shows an analysis of the influence of the amount of jitter (panel A) and the duration of the digital blanking (panel B) on the number of averaged samples along the averaging window of an ABR signal (10 ms) with the RSA method. The stimulation sequences of this study were generated using 20 000 stimuli randomly distributed with a uniform distribution of probability between "a" and "b" ms ($ISI_{a–b}$). Analysis of panel A shows the influence of the amount of jitter on the number of averaged samples when the duration of digital blanking is 1 ms. In this analysis, using a 4 ms jittered stimulation sequence ($ISI_{5–9}$), the lowest number of averaged samples is around 15 000 samples; in a 2 ms jittered sequence ($ISI_{5–7}$), that number is about 10 000 samples; and in a 0.5 ms jittered sequence ($ISI_{5–5.5}$), there would be a segment in the averaging window that could not be obtained. Analysis of panel B shows the influence of long- and short-duration blanking on the number of averaged samples along the averaging window. This analysis shows that long duration blanking used in long duration stimuli would impose the restriction of a large amount of jitter to meet the requirement of averaging at least 70% of the available samples. The use of a shorter-duration blanking could allow less jittered stimulation sequences to be implemented. This study shows that the amount of jitter and the duration of digital blanking are parameters influencing the number of averaged samples along the averaging window. The RSA method requires (a) a minimum amount of jitter that must be greater than the dominant period of the components of the AEPs to allow positive and negative components of the interference associated with overlapping responses to be canceled by averaging, and (b) a jitter distribution that allows a sufficient number of averaged samples all along the averaging window to avoid appreciable differences in quality between different segments of the recorded AEP.

With the above limitations of RSA in mind, the authors have developed a modified version of RSA which does not require a digital blanking process and eliminates the interference associated with overlapping adjacent responses through an iterative process in the time domain. We have called this approach I-RSA. This version of RSA maintains the main properties of RSA, while overcoming the limitation of the jitter imposed in RSA. The approach for this method is based on iterations that include estimation of the interference associated with overlapping responses, its subtraction from the recorded EEG, and re-estimation of the AEP. The improved AEP estimate on each iteration leads to a better estimate of the interference associated with overlapping responses, and a better AEP estimate can therefore be obtained recursively. The accuracy of the AEP estimate increases with the number of iterations. The total number of iterations can be set either as a predefined value, or automatically, in which case the method stops iterating when the differences between AEP estimates in successive iterations are negligible. As in RSA, the generation of stimulation sequences in I-RSA is based on randomized stimulation, where the ISI of the stimuli varies randomly according to a predefined probability distribution (Valderrama *et al.*, 2012).

The mathematical formulation of I-RSA is described below. Using RSA notation (Valderrama *et al.*, 2012), the estimate of the transient evoked potential $\hat{x}(j)$ $(j = 1,\ldots, J)$ is obtained in I-RSA by an iterative process in the time domain. Each iteration (i) results in an estimate of the transient evoked potential, represented by $\widehat{h}_i(j)$. The AEP estimate in each iteration by the I-RSA method is obtained as the average of the K sweeps, in which the contribution of the adjacent responses to each current response is suppressed,

$$\widehat{h}_i(j) = \frac{1}{K}\sum_{k=1}^{K} y_k\big(j + m(k)\big), \quad (5)$$

where $y_k(n)$ $(n = 1,\ldots,N)$ represents the EEG in which the kth response is kept, but all the other responses (i.e., the

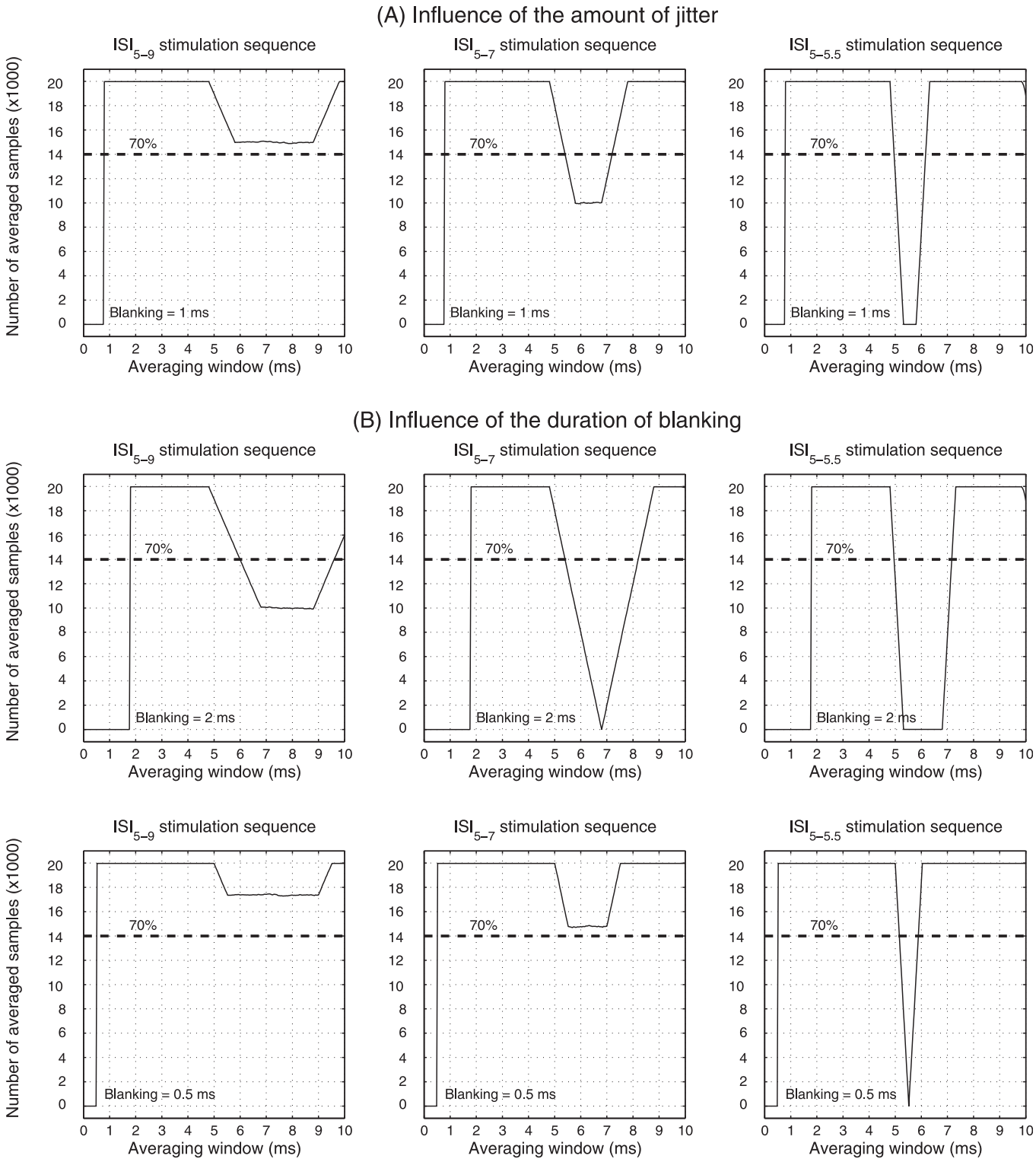

FIG. 2. Influence of the amount of jitter of the stimulation sequence (panel A) and the duration of digital blanking (panel B) on the number of samples averaged along the averaging window for an ABR signal with the RSA method. This figure shows that low-jittered sequences and long-duration blanking can produce appreciable differences in terms of quality between different segments of the response.

overlapping responses) are subtracted. The $y_k(n)$ signals can be obtained for each stimulus as the original electroencephalogram $y(n)$ minus the AEP estimates on the preceding iteration $\hat{h}_{i-1}$ corresponding to all stimuli excluding the stimulus k,

$$y_k(n) = y(n) - (s(n) - s_k(n)) * h_{i-1}, \tag{6}$$

where $s_k(n)$ represents the stimulation signal for the stimulus k, and the symbol $*$ is the convolution operator. Considering the signal $z(n)$ as the original EEG with all AEPs suppressed: $z(n) = y(n) - s(n) * h_{i-1}$, then

$$\begin{aligned} y_k(n) &= y(n) - s(n) * h_{i-1} + s_k(n) * h_{i-1} \\ &= z(n) + s_k(n) * h_{i-1}. \end{aligned} \tag{7}$$

The sections of y_k corresponding to the averaging window of the stimulus k can thus be obtained as

$$y_k(j+m(k)) = z(j+m(k)) + s_k(j+m(k)) * h_{i-1}. \quad (8)$$

The $s_k(n)$ signal can be represented as $\delta(n - m(k))$, where $\delta(n)$ represents the Dirac delta function, with the value 1 for $n=0$, and 0 otherwise. Hence

$$\begin{aligned} y_k(j+m(k)) &= z(j+m(k)) + \delta(j+m(k) - m(k)) * h_{i-1} \\ &= z(j+m(k)) + h_{i-1}, \end{aligned} \quad (9)$$

since $\delta(j) * f = f$ for whatever function f. Therefore, Eq. (5) can be rewritten as

$$\begin{aligned} \widehat{h}_i(j) &= \frac{1}{K}\sum_{k=1}^{K}\left[z\left(j+m(k)\right) + h_{i-1}\right] \\ &= h_{i-1} + \frac{1}{K}\sum_{k=1}^{K}\left[z\left(j+m\,(k)\right)\right]. \end{aligned} \quad (10)$$

In this equation, the term $(1/K)\sum_{k=1}^{K} z(j+m(k))$ represents the correction made to the AEP estimate on the preceding iteration h_{i-1}. Under certain jitter distributions and stimulation rates, this correction parameter may cause instability problems, leading to worse AEP estimates in successive iterations. We have verified (with simulations and real ABR and MLR signals) that problems of instability usually arise with narrow distributions of the jitter and stimulation rates in which the averaged ISI is close to a maximum value of the AEP autocorrelation function. The instability issue can be solved by inserting a correction factor α, which may constrain (α-values lower than 1) or enhance (α-values greater than 1) the correction made to h_{i-1}. Thus, the AEP estimate in iteration i is obtained as

$$\widehat{h}_i(j) = h_{i-1} + \alpha \cdot \frac{1}{K}\sum_{k=1}^{K}\left[z\left(j+m\,(k)\right)\right]. \quad (11)$$

The value of the α parameter can be defined either as a fixed value in all iterations or adaptive in each iteration. Theoretically, the optimal α-value is the greatest value of α that avoids instability. Greater α-values would provide increasing oscillations in successive iterations, leading to an unstable solution. Lower α-values slow down the speed of convergence toward the AEP estimate, even though convergence would be guaranteed. An adaptive definition of α-value could be an efficient alternative, in which the value of α increases or decreases in each iteration according to a diagnosis of convergence.

The estimated AEP on each iteration $\widehat{h}_i(j)$ is used in the following iteration as $\widehat{h}_{i-1}(j)$. The I-RSA method is initialized with $\widehat{h}_0(j) = 0\ \forall j$. Finally, the estimate of the transient AEP by I-RSA $\hat{x}(j)$ can be obtained either as the estimated AEP after a predefined number of iterations I ($\hat{x}(j) = \widehat{h}_I(j)$), or when the differences between the AEP estimates in successive iterations are negligible ($\hat{x}(j) = \widehat{h}_i(j)$ if $\widehat{h}_i(j) \approx \widehat{h}_{i-1}(j)$).

Figure 3 illustrates an example of an iteration of the I-RSA method outlined above. In this example, the sampling frequency is $f_s = 25$ kHz, the length of the averaging window is $J = 2500$ samples, which corresponds to 100 ms, and the correction factor is $\alpha = 1$. Figure 3(A) shows an MLR signal as an example of transient AEP. The ABR, N_a, P_a, N_b, and P_b components can be identified in this transient AEP. Figure 3(B) shows a segment of a synchronization signal $s(n)$ whose interstimulus intervals vary randomly with a uniform distribution between 42 and 58 ms (ISI_{42-58}). The index of the samples at which stimuli start $m(k)$ ($k = 1,\ldots,5$) are

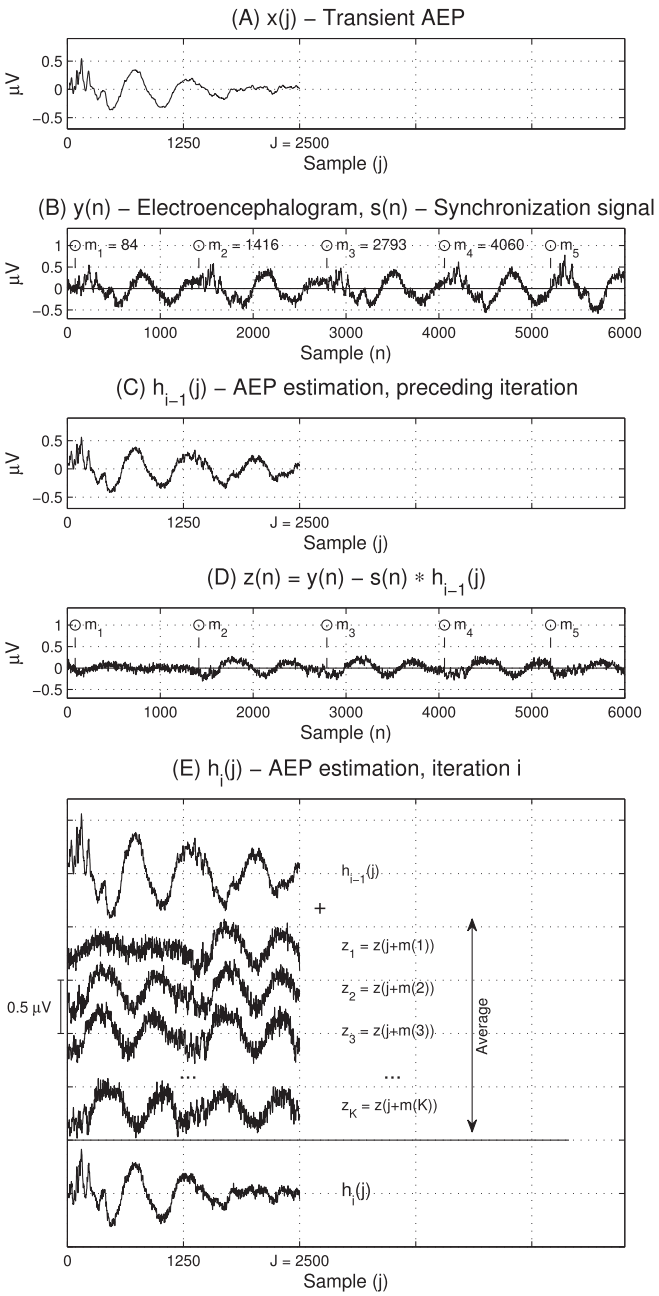

FIG. 3. An illustration of estimation of the AEP based on I-RSA. Sampling frequency: $f_s = 25$ kHz; length of the averaging window: $J = 2500$ samples (100 ms); correction factor: $\alpha = 1$. (A) Transient AEP. This example shows a MLR signal. (B) Synchronization signal and raw EEG (in this example, the EEG was synthesized from a real MLR response). (C) Estimation of the AEP on the preceding iteration. (D) EEG with all overlapping responses subtracted. (E) Estimation of the AEP on the iteration i.

shown next to each stimulus. This figure also shows the recorded EEG, which in this example was artificially synthesized by the convolution of the synchronization signal and the transient AEP plus white noise added to the EEG at a SNR of 9.5 dB. Figure 3(C) shows the estimated AEP on the preceding iteration: $h_{i-1}(j)$, which is used in the iteration i as an approximation of the AEP to evaluate and suppress the interference associated with overlapping responses. Figure 3(D) shows the recorded EEG with all overlapping responses subtracted ($z(n)$). Figure 3(E) outlines the AEP-estimation process for the iteration i, which is obtained by adding the AEP estimation in the preceding iteration $h_{i-1}(j)$ to the average of the signals $z_1 \cdots z_K$.

The performance of the RSA and I-RSA methods is assessed in this paper with both real and artificially synthesized ABR and MLR signals using stimulation sequences of different rates and jitter distributions.

B. EEG recording

The AEP-recording procedure consisted of the presentation of auditory stimuli to the subjects and the recording of their associated electrical responses (sweeps). Stimulation of the auditory system was performed monaurally by monophasic 0.1 ms rarefaction clicks to evoke a synchronous firing of neurons, especially those in the 1000–4000 Hz region (Hall, 2007; Thornton, 2007), using an insert earphone (ER-3A Etymotic Research, Elk Grove Village, IL). The recording sessions took place in a shielded screening booth prepared to attenuate acoustical and electromagnetic interference. The subjects were seated comfortably in order to minimize electromyogenic interference. The intensity level 0 dB normal-hearing level (nHL) corresponds to 33.54 dB peak-to-peak equivalent sound pressure level dB pe-SPL, calibrated by an Artificial Ear type 4153 2-cc acoustic coupler (Brüel & Kjær Sound & Vibration Measurement A/S, Nærum, Denmark). The EEGs were recorded by Ag/AgCl surface electrodes placed on the upper forehead (active), lower forehead (ground), and ipsilateral mastoid (reference). The interelectrode impedance was below 5 kΩ in all recordings. The EEG was amplified by 70 dB and bandpass filtered by a 24 dB/Octave slope filter with a bandwidth of [150–3500] Hz for ABR and [0.5–3500] Hz for MLR. The recorded signal was sampled at 25 kHz, digitally filtered (fourth order, bandwidth: [300–3000] Hz for ABR, [30–1000] Hz for MLR), and stored using 16 bits of quantization. Digital signals were processed with algorithms implemented in MATLAB (The Mathworks, Inc., Natick, MA). An artifact-rejection method prevented the processing of any sweeps whose maximum amplitude exceeded $\pm 10\,\mu$V. No recordings were processed from the first second of the recording test in order to acclimatize the subject to the stimulation sequence and prevent the processing of any ERPs associated with novelty. A fuller description of the recording system used in this study can be found in Valderrama *et al.* (2011, 2014c).

The recording process carried out in this study was in accordance with the Code of Ethics of the World Medical Association (Declaration of Helsinki) for experiments involving humans, and it was approved by the Research Ethics Committee established by the Health Research Authority (Reference No. RHM ENT0082).

C. Description of the experiments

This study involves the recording of ABR and MLR signals at different stimulation rates using RSA and I-RSA methods. Sixteen subjects, 10 males and 6 females, aged 19–46 yrs (with a mean and standard deviation age of 30 ± 6) were recruited for this study. No participant showed any significant auditory dysfunction, presenting audiometric thresholds of 20 dB hearing level or less for pure tones between 250 and 8000 Hz. The subjects were volunteers and were informed in detail about the experimental protocol and possible side effects of the test. A consent form was signed by the participants before the beginning of the recording session, which was carried out at the Royal South Hants Hospital (Southampton, United Kingdom). Subjects #S1 to #S8 participated in the study of ABR signals, and subjects #S9 to #S16 participated in the study of MLR signals. The RSA and I-RSA methods were implemented as presented in Sec. II A of this paper. In RSA, the digital blanking used in the RSA method was 1 ms ([−0.2 to 0.8] ms). The randomized stimulation sequences used in this study were built according to uniform jitter distributions, i.e., the ISI of an ISI_{a-b} stimulation sequence varies randomly with uniform distribution between "a" and "b" ms (Valderrama *et al.*, 2012).

The first experiment consists of a study of the interference associated with overlapping responses in both real and computer simulated ABR and MLR signals obtained at different stimulation rates with the RSA and I-RSA methods in different jittering conditions. The aim of this study is to assess the performance of the proposed method (I-RSA), and to analyze the effects of the interference associated with overlapping responses with ABR and MLR signals obtained from the RSA and I-RSA methods when the amount of jitter is greater than, equal to, and shorter than the dominant period of the ABR/MLR components. In this experiment, the I-RSA method was implemented using an adaptive α-value and a large number of iterations ($I = 1000$) in order to achieve convergence in all scenarios. The adaptive definition of α in each iteration consisted of increasing α-value at a 10% factor in case of convergence, and decreasing its value at a 40% factor in case of instability. Convergence or instability was verified by comparing the energy of the correction factor at the current iteration with that of the preceding iteration (an increase is a symptom of instability). The value of α in the first iteration was 0.8.

The study of ABR signals included the generation of stimulation sequences at rates of 71 Hz (8500 stimuli), 83 Hz (10 000 stimuli), 100 Hz (12 000 stimuli), 125 Hz (15 000 stimuli), 167 Hz (20 000 stimuli), 250 Hz (30 000 stimuli), and 300 Hz (36 000 stimuli), using jitter distributions greater than (4 ms), equal to (2 ms), and shorter than (0.6 ms) the

dominant period of the ABR components (about 2 ms). The recording of MLR signals was performed by generating stimulation sequences at rates of 8 Hz (2000 stimuli), 20 Hz (2400 stimuli), 40 Hz (4800 stimuli), 67 Hz (8000 stimuli), 100 Hz (12 000 stimuli), and 125 Hz (15 000 stimuli), using jitter distributions greater than (50 ms), equal to (25 ms), and shorter than (16 ms) the dominant period of the MLR components (about 25 ms). The varying number of stimuli used in these stimulation sequences was set to achieve a compromise between the duration of the test and the quality of the response. An averaging window of 25 ms ($J = 625$ samples) was used in the study of ABR signals to expand the analysis of the interference associated with overlapping adjacent responses outside the standard averaging window (10 ms). The length of the averaging window for MLR signals was 100 ms ($J = 2500$ samples). In the study with computer-simulated signals, real high-quality ABR and MLR signals were used as templates. The template used for the ABR test was recorded from subject #S8 (male, aged 26), using 20 000 stimuli presented at 70 dB nHL with a stimulation sequence $ISI_{20–24}$ (45 Hz). The template used for the MLR test was recorded from subject #S9 (male, aged 28), with stimuli presented at 70 dB nHL using a stimulation sequence $ISI_{117–133}$ (8 Hz) of 10 000 stimuli. Different EEGs were artificially synthesized by the convolution of the templates with each stimulation sequence of this study. An estimate of the template was obtained by the RSA and I-RSA methods from the EEG synthesized at each stimulation rate and under each jittering condition. The advantage for using artificially synthesized EEGs is that they do not include any noise artifacts typically present in the recording of real AEPs, such as interference derived from the myogenic activity of the subject or from electromagnetic interference. The only type of interference included in these synthesized EEGs is associated with overlapping responses, which was estimated as the root-mean-square (rms) value of the difference between the template and the signals obtained by each method. Furthermore, in simulation, the original ABR/MLR template is known, which allows determining the effects of overlapping responses in the ABR/MLR estimates by the RSA and I-RSA methods. In the study with real signals, the ABR and MLR signals were recorded from subject #S9 (male, aged 28) using stimuli presented at 70 dB nHL. The real ABR and MLR signals were obtained from these recorded EEGs using the RSA and I-RSA methods.

The second experiment includes an analysis of latencies and amplitudes of the peaks of real ABR and MLR signals obtained with RSA and I-RSA at different stimulation rates in a set of 8 normal-hearing subjects for the study of ABR signals (6 males and 2 females, aged 16–36), and a different set of 8 normal-hearing subjects for the study of MLR signals (4 males and 4 females, aged 23–46). In this experiment, the I-RSA method was implemented using fixed values of $\alpha = 0.8$ and $I = 50$ iterations. ABR signals were elicited by stimuli presented at 70 dB nHL at rates of 45, 56, 71, 83, 100, 125, and 250 Hz (20 000 stimuli in all rates), using jitter distributions of 4 ms (greater than the dominant period of the ABR components). MLR signals were elicited by stimuli presented at 70 dB nHL at the rates 8 Hz (2000 stimuli), 20 Hz (5000 stimuli), 40 Hz (5000 stimuli), 67 Hz (5000 stimuli), 100 Hz (10 000 stimuli), and 125 Hz (20 000 stimuli), using jitter distributions of 16 ms (shorter than the dominant period of the MLR components). The varying number of stimuli used in the stimulation sequences allowed MLR signals of sufficient quality to be recorded with an appropriate recording time. The length of the averaging window was 10 ms for ABR signals ($J = 250$ samples), and 100 ms for MLR signals ($J = 2500$ samples). Latencies (L_{peak}) were measured as the difference in milliseconds between the stimulus onset and the maximum value of the peak. In ABR signals, amplitudes (A_{peak}) were measured in microvolts as the difference between the top of the peak and the following trough; whereas in MLR signals, amplitudes were measured as the difference between the negative and positive wave complex (Hall, 2007; Burkard and Don, 2007; Pratt, 2007).

The differences between the morphology of the AEPs obtained with the RSA and I-RSA methods were analyzed by a matched paired *t*-test for differences in latencies (L_{RSA}-$L_{I\text{-}RSA}$) and by a matched paired Wilcoxon signed rank test for the ratio of amplitudes calculated as $A_{RSA}/A_{I\text{-}RSA} - 1$, using a significance level of $\alpha = 0.05$ in both analyses.

III. RESULTS

A. Experiment 1

Figure 4 shows real and computer-simulated ABR (panel A) and MLR (panel B) signals obtained with the RSA and I-RSA methods at different rates using stimulation sequences of jitter distributions greater than, equal to, and shorter than the dominant period of the ABR/MLR components. In ABR signals, the averaging window of 25 ms allows the interference associated with overlapping adjacent responses to be studied outside the standard averaging window for ABR signals (10 ms). In the computer-simulated study, the signals used as a template are shown below each figure. The main components of these AEPs are labeled on the figure. The level of interference associated with overlapping responses has been estimated in each method as the rms value of the difference between the template and the obtained signals by the RSA and I-RSA methods. The study with simulated signals shows that estimation of the ABR and MLR signals by the RSA method is accurate when the distribution of the jitter is greater than the dominant period of the ABR/MLR components. The ABR signals corresponding to a jitter distribution of 4 ms and the MLR signals corresponding to a jitter distribution of 50 ms present a similar morphology to their corresponding template (with similar latencies and amplitudes of their components). When the jitter distribution is equal to the dominant period of the ABR/MLR components, i.e., jitter of 2 ms for ABRs and 25 ms for MLRs, the ABR and MLR signals estimated by the RSA method present small differences with the template waveform owing to the interference associated with overlapping responses. For instance, some additional peaks appear outside the averaging window in ABR signals, and the components wave I at 125 Hz; wave II at 167 Hz; waves I, III, and VII at 250 Hz; and the P_b at 20 Hz are slightly overestimated. The effects of interference associated with overlapping responses become particularly manifest when the jitter is

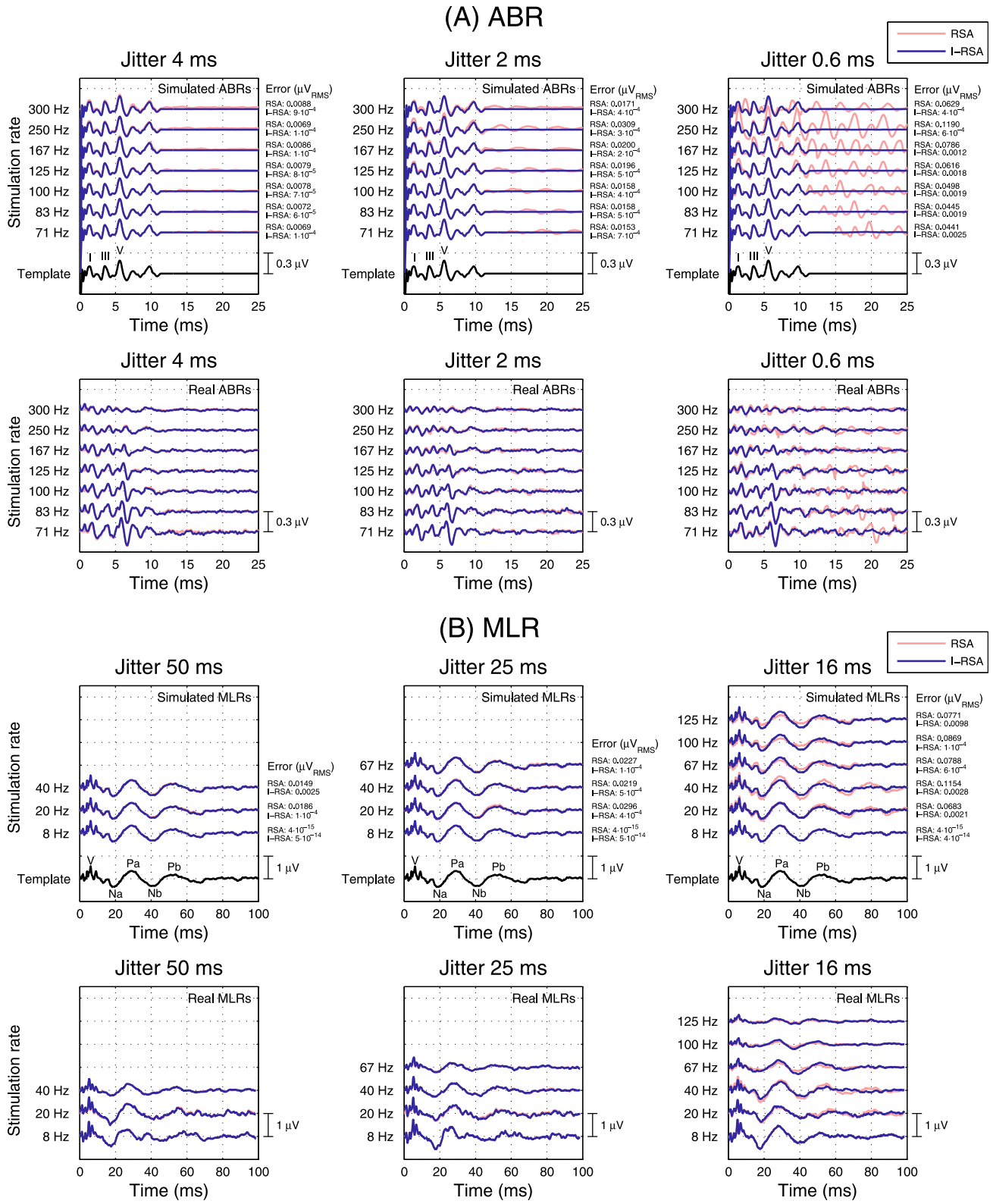

FIG. 4. (Color online) Real and computer-simulated ABR (panel A) and MLR (panel B) signals obtained with RSA and I-RSA at different stimulation rates using stimulation sequences of jitter distributions that are greater than, equal to, and shorter than the dominant period of the ABR/MLR components. In the study with simulated ABR/MLR signals, the interference associated with overlapping responses has been estimated as the rms value of the difference between the template and the signals obtained.

shorter than the dominant period of the ABR/MLR components, e.g., jitter of 0.6 ms for ABRs and 16 ms for MLRs. At rates up to 100 Hz, the ABR signals estimated by RSA perfectly fit the template waveform, although a discernible waveform similar in morphology to an ABR signal appears next to the response (between 10 and 25 ms) owing to the interference associated with overlapping responses. As the stimulation rate increases, these additional components

(which are due to interference, and are not part of the true response) appear on the latencies of ABR components (first 10 ms) and produce contamination of the response, which cannot be reduced by averaging. Some of these effects are overestimation of waves I and VII at 125 Hz; waves III, VI, and VII at 167 Hz; waves I, V, and VII at 250 Hz, and wave II at 300 Hz. Additionally, this figure shows that the ABR signals obtained for a jitter of 0.6 ms present noticeable differences in quality between different segments of the response, and certain segments could not be obtained as a result of digital blanking.

Analysis of the effects of overlapping responses in MLR signals shows significant differences between the MLRs obtained with RSA and the template. At 20 Hz, these effects cause overestimation of the P_b component and the generation of an additional peak at about 80 ms. At 40 Hz, the effects of overlapping responses cause significant overestimation of the N_a, P_a, N_b, and P_b components, and an additional peak is also generated at latency of about 80 ms. These effects are a consequence of the resonance generated when the components are in phase (occurring at the same time relative to the stimulus) and overlap (Bohorquez and Ozdamar, 2008). This phenomenon is generally known as 40-Hz ERP and was first described by Galambos *et al.* (1981). The latencies of the components are estimated correctly at rates of 20 and 40 Hz. At rates of 67, 100, and 125 Hz the interference associated with overlapping responses causes underestimation of the amplitudes of all components. Underestimation of the amplitude of the P_b component at these rates leads to premature estimation of its latency. In contrast to RSA, the computer-simulated study shows that the I-RSA method is able to estimate the true AEP (template) accurately under all recording conditions. The ABR and MLR signals obtained by the I-RSA method present the same morphology as the template signal, and the interference associated with overlapping responses in I-RSA is lower than 0.01 μV_{rms} for all ABR and MLR signals at all stimulation rates and under all jittering conditions.

Analysis of the morphology of real ABR and MLR signals obtained with the RSA and I-RSA methods is consistent with the computer-simulated study. This study shows no significant differences between the ABR and MLR signals obtained with the RSA and I-RSA methods when the jitter of the stimulation sequences is greater than (4 ms for ABRs and 50 ms for MLRs) or equal to (2 ms for ABRs and 25 ms for MLRs) the dominant period of the ABR/MLR components. The real ABR signals obtained with RSA for a jitter of 0.6 ms at rates of 71, 83, 100, and 125 Hz show additional components similar in morphology to ABR signals appearing with latencies of 10–25 ms. At rates higher than 100 Hz these additional components (which are not part of the response) appear within the first 10 ms of the averaging window and contaminate the response, producing, for example, overestimation of wave I at 125 Hz, of wave II at 167 Hz, and of wave IV at 250 Hz. In contrast, the ABR signals obtained with the I-RSA method present no additional components, and the changes in the morphology of the ABR signals across stimulation rates is consistent with previous literature: As the stimulation rate increases, the amplitude of the components decreases and the latency increases (to a greater extent the more central the components) as a consequence of neural adaptation (Lasky, 1997; Burkard *et al.*, 1990; Valderrama *et al.*, 2014a).

The real MLR signals obtained with RSA and I-RSA for a jitter of 16 ms show discernible differences consistent with the computer-simulated analysis. Taking the signals obtained with I-RSA as a reference, the P_b component on the MLR signal obtained with RSA at 20 Hz is overestimated, the N_a-P_a and N_b-P_b components are overestimated at 40 Hz, and the N_a-P_a and N_b-P_b components are underestimated at rates of 67, 100, and 125 Hz.

These results highlight that (a) the performance of the RSA method is appropriate when the jitter of the stimulation sequence is greater than the dominant period of the ABR/MLR components, and (b) the I-RSA method is able to suppress the interference associated with overlapping responses, leading to accurate estimates of ABR and MLR signals when the jitter is either greater or shorter than the dominant period of the ABR/MLR components.

B. Experiment 2

Figure 5 shows ABR (panel A) and MLR (panel B) signals recorded on 2 sets of 8 normal-hearing subjects (16 participants) at different stimulation rates with the RSA and I-RSA methods. Overlapping the AEPs recorded with the RSA and I-RSA methods under each recording condition allows their differences to be appreciated. This experiment includes an analysis of amplitudes and latencies of ABR and MLR signals obtained by both methods.

Figure 6 shows the mean (and standard deviation in error bars) of the latencies and amplitudes of the main components of ABR (panel A) and MLR (panel B) signals obtained by the RSA and I-RSA methods at different stimulation rates. The values of these parameters estimated in both ABR and MLR signals by the I-RSA method are consistent with other studies reporting AEPs obtained using the MLS and CLAD methods (Lasky, 1984; Lina-Granade *et al.*, 1993; Leung *et al.*, 1998; Stone *et al.*, 2009; Bell *et al.*, 2001, 2002; Ozdamar *et al.*, 2007). The large standard deviation of the analysis of amplitudes in this study points toward significant variability among subjects in terms of amplitudes. With regard to ABR signals, the analysis of latencies and amplitudes of waves I, III, and V indicates that as the stimulation rate increases: (a) The latency of wave I experiences a slight positive shift, (b) the latency of wave III undergoes a moderate positive shift, (c) the latency of wave V increases in more deeply, and (d) the amplitude of all the waves decreases. The deeper shift of wave V in comparison with wave III highlights that the stimulation rate influences central components to a greater extent than peripheral components, which is consistent with previous studies (Pratt and Sohmer, 1976; Yagi and Kaga, 1979; Jiang *et al.*, 2009). The analysis of latencies and amplitudes of MLR signals obtained with the I-RSA method at different stimulation rates shows that as stimulation rate increases: (a) The latency of the N_a and P_a components remains fairly constant, (b) the latency of the N_b and P_b components decreases, (c) the

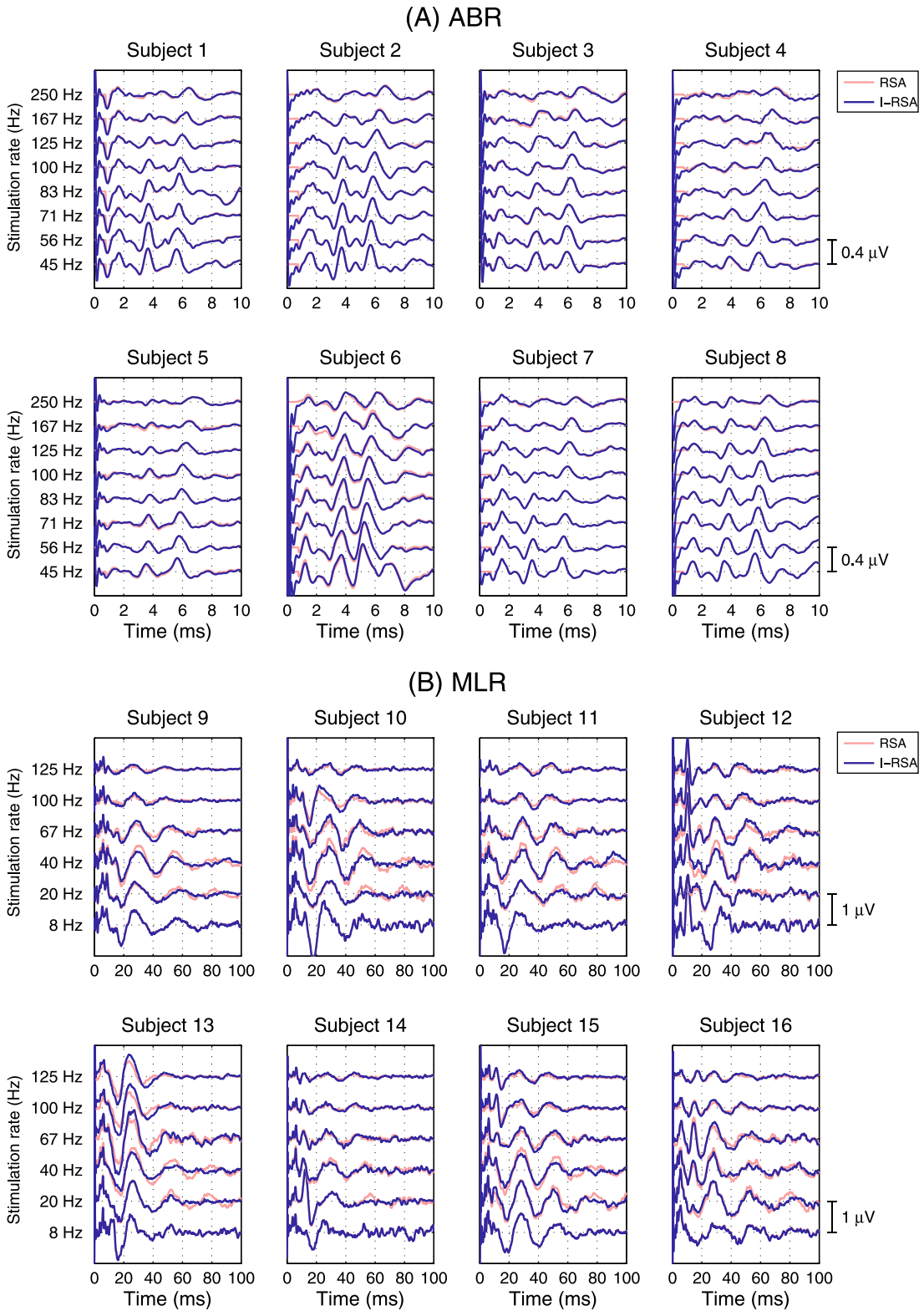

FIG. 5. (Color online) Panel A: ABR signals obtained in a set of eight normal-hearing subjects at different stimulation rates obtained by RSA and I-RSA using stimulation sequences of a jitter of 4 ms (greater than the dominant period of ABR components). Panel B: MLR signals obtained in a different set of eight normal-hearing subjects at different stimulation rates obtained by RSA and I-RSA using stimulation sequences of a jitter of 16 ms (lower than the dominant period of MLR components).

amplitude of the N_a-P_a component decreases, and (d) the amplitude of the N_b-P_b component increases at 40 and 67 Hz and decreases at other rates. The resonance of the N_b-P_b amplitude at 40 and 67 Hz is possibly due to the association of this component with the auditory primary thalamo-cortical pathway at low rates, and with the non-primary reticulo-thalamo-cortical pathway at rates near 50 Hz (Ozdamar *et al.*, 2007).

A comparison of the latencies and amplitudes of AEPs obtained by the RSA and I-RSA methods is shown in

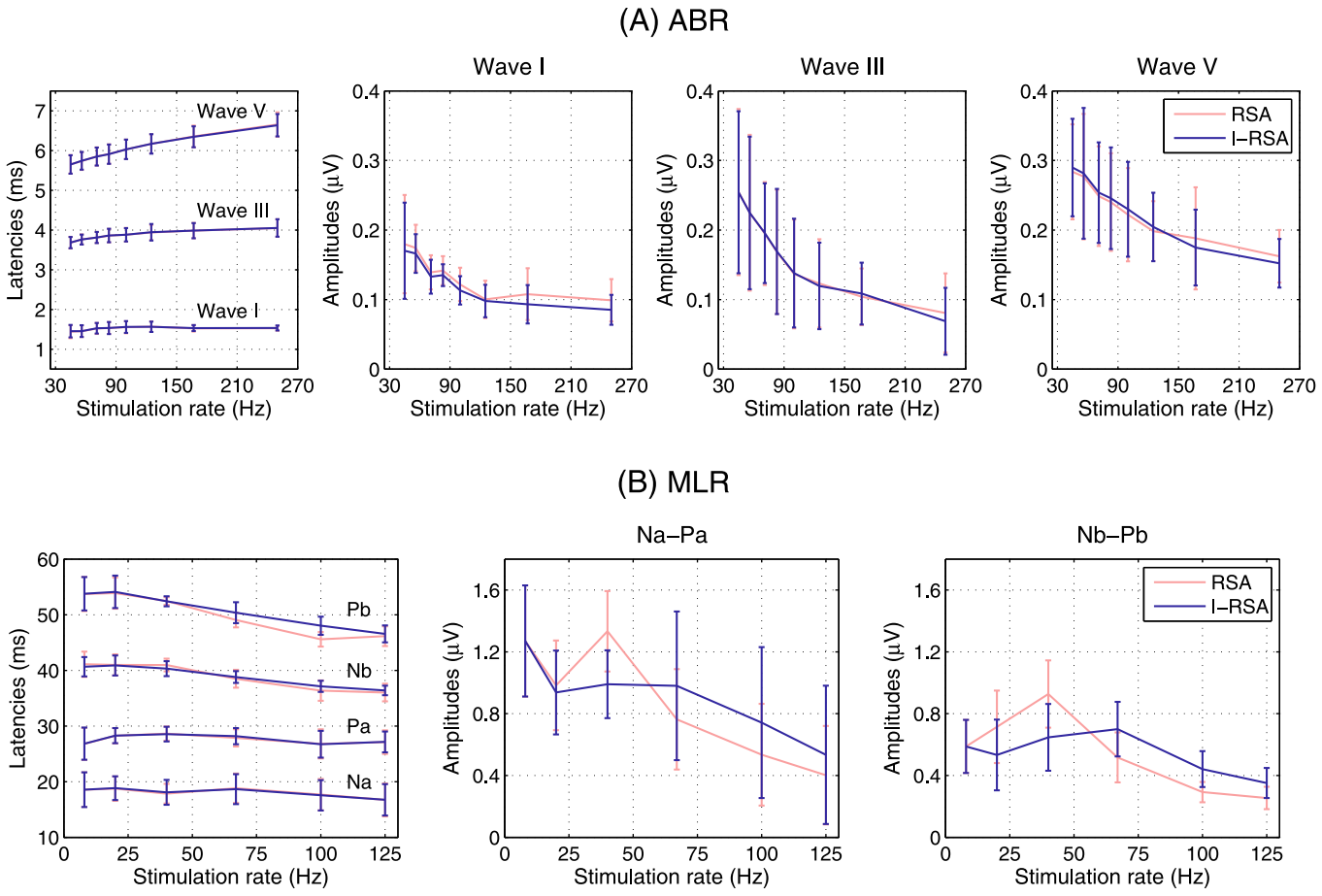

FIG. 6. (Color online) Mean (and standard deviation in error bars) of the latencies and amplitudes of the main components of ABR (panel A) and MLR (panel B) signals obtained by the RSA and I-RSA methods at different stimulation rates.

Tables I and II. These tables show the mean (and standard deviation in parentheses) of the differences of latencies expressed in milliseconds (L_{RSA}-$L_{I\text{-}RSA}$) and ratio of amplitudes (estimated as $A_{RSA}/A_{I\text{-}RSA} - 1$) between AEPs obtained by the RSA and I-RSA methods. Asterisks represent statistically significant differences between the two methods (*: p-value < 0.05; **: p-value < 0.01). The results shown in Table I indicate that measurements of L_I, L_{III}, and L_V by the RSA and I-RSA methods are very similar, with maximum absolute differences of 0.02 ms between both estimates (on average). This analysis also shows that the differences between estimates of A_I, A_{III}, and A_V by the two methods are less than 10%, except for the estimation of A_I at 167 and 250 Hz, and A_{III} at 250 Hz, in which RSA overestimates the amplitude by a factor of 15%, 14%, and 18%, respectively. The same analysis with MLR signals (Table II) reveals that the latency estimates for all parameters at all stimulation rates obtained by the RSA and I-RSA are comparable. Only the estimation of L_{P_b} at 100 Hz shows statistically significant differences of 2.44 ms, on average, between the two methods. In contrast, analysis of $A_{N_a-P_a}$ and $A_{N_b-P_b}$ shows significant differences between the estimates of these parameters by the two methods. Taking the signals obtained with I-RSA as a reference, at 20 Hz, there are no significant differences in the estimation of $A_{N_a-P_a}$, but RSA overestimates $A_{N_b-P_b}$ by a factor of 41%, on average. At 40 Hz, RSA overestimates both $A_{N_a-P_a}$ and $A_{N_b-P_b}$ by a factor of 36% and 48%, respectively, as a consequence of the overlapping of the resonating P_b component on the P_a component (Bohorquez and Ozdamar, 2008). At 67 Hz and greater rates, RSA produces a statistically significant underestimation of both $A_{N_a-P_a}$ and $A_{N_b-P_b}$ parameters of greater than 20%. The results of this analysis are presented in graphic form in Figs. 5 and 6.

IV. DISCUSSION

The RSA method consists in the average of auditory responses corresponding to a burst of stimuli whose ISI varies randomly according to a predefined probability distribution along the entire stimulation sequence (randomized stimulation). This method includes a digital blanking process that considers as null values any EEG samples contaminated by the stimulus artifact (Valderrama *et al.*, 2012). Digital blanking entails non-uniform averaging of responses along the averaging window, which can lead to significant differences in quality between different segments of the response if the amount of jitter is not sufficiently large. The average of at least 70% of the available responses assures differences of quality of less than 1.55 dB, which may be appropriate for many applications. Long-duration blanking used for long-duration stimuli (e.g., windowed tones) would impose the

TABLE I. Mean (and standard deviation in parentheses) of the differences in latencies expressed in milliseconds (L_{RSA}-$L_{I\text{-}RSA}$) and the ratio of amplitudes (estimated as $A_{RSA}/A_{I\text{-}RSA} - 1$) between ABR signals obtained by the RSA and I-RSA methods. Statistically significant differences between the two methods are expressed with asterisks (*: p-value < 0.05; **: p-value < 0.01).

Stimulation rate	L_I	L_{III}	L_V	A_I	A_{III}	A_V
45 Hz	−0.01 (0.02)	0.00 (0.00)	0.00 (0.01)	0.05 (0.04)*	0.00 (0.01)	−0.02 (0.02)**
56 Hz	0.00 (0.00)	0.00 (0.01)	−0.01 (0.00)*	0.05 (0.05)*	0.00 (0.01)	−0.02 (0.01)**
71 Hz	0.00 (0.01)	0.00 (0.01)	0.00 (0.01)	0.05 (0.04)	−0.01 (0.01)	−0.02 (0.01)**
83 Hz	0.00 (0.01)	0.00 (0.01)	0.00 (0.00)	0.05 (0.05)	0.00 (0.01)	−0.02 (0.01)**
100 Hz	−0.01 (0.01)*	0.00 (0.01)	0.00 (0.00)	0.07 (0.05)*	−0.01 (0.02)*	−0.04 (0.03)**
125 Hz	0.00 (0.01)	−0.01 (0.02)	0.00 (0.01)	0.02 (0.06)	0.03 (0.06)	−0.02 (0.07)
167 Hz	0.00 (0.01)	0.00 (0.01)	0.01 (0.03)	0.15 (0.14)	−0.03 (0.13)	0.06 (0.07)
250 Hz	0.00 (0.01)	0.00 (0.01)	0.02 (0.05)	0.14 (0.10)	0.18 (0.17)	0.07 (0.05)*

restriction of more jitter in order to meet this requirement, which could restrict the implementation of this method in certain scenarios. Moreover, as RSA does not perform deconvolution, this method must deal with interference derived from overlapping adjacent responses. This type of interference can be reduced by averaging provided that the jitter of the stimulation sequence is large enough, thus enabling positive and negative components of this interference to be canceled out. When the premise of a minimum amount of jitter is fulfilled, RSA has proved to be effective in recording ABR signals at high stimulation rates (Valderrama *et al.*, 2012, 2014a,b, 2014c).

The purpose of this paper was to analyze the effects of interference associated with overlapping responses in ABR and MLR signals recorded at different rates with randomized stimulation sequences whose jitter distributions were greater and lower than the dominant period of the ABR/MLR components. In addition, this paper has presented the I-RSA method, a new approach of RSA that estimates and subtracts the interference associated with overlapping responses through an iterative process in the time domain. The iterative procedure of the I-RSA method can derive into problems of instability under certain distributions of the jitter and stimulation rates, leading to worse AEP estimates in successive iterations. Instability is a common problem that is also present in methods based in deconvolution [these methods must define stimulation sequences whose frequency components are not close to zero to avoid noise amplification (Jewett *et al.*, 2004; Ozdamar and Bohorquez, 2006; Bardy *et al.*, 2014a)]. The instability sometimes observed in I-RSA is associated to the fact that I-RSA performs some kind of deconvolution in the time domain [like in the case of ADJAR (Woldorff, 1993)]. In contrast to ADJAR, I-RSA provides a procedure to avoid instability by including the α-parameter in the correction.

Two experiments were performed in this study with the dual purpose of (a) analyzing the effects of the interference derived from overlapping responses in ABR and MLR signals obtained at different rates by the RSA and I-RSA methods, using stimulation sequences of a jitter greater and shorter than the dominant period of the ABR/MLR components, and (b) validating the I-RSA method proposed to record ABR and MLR signals at high stimulation rates.

In the first experiment, the study with simulated signals showed that the RSA method accurately estimated the templates in ABR and MLR signals at all rates when the jitter was larger than the dominant period of the ABR/MLR components, indicating that the RSA method was able to reduce the effects of the interference associated with overlapping responses with averaging. However, when the jitter was shorter than the dominant period of the ABR/MLR components, this analysis revealed significant differences between the template and the signals estimated by RSA as a consequence of interference associated with overlapping responses. Additionally, the use of blanking of 1 ms duration and a jitter of 0.6 ms produced significant differences in quality between different segments of the response, and certain segments could not be obtained because of the limitation imposed by the digital blanking process. These results indicate that estimation of the AEP by the RSA method is not reliable when the jitter of the stimulation sequence is shorter than the dominant period of the ABR/MLR components, since the interference associated with overlapping responses cannot be reduced by averaging. According to the I-RSA

TABLE II. Mean (and standard deviation in parentheses) of the differences in latencies expressed in milliseconds (L_{RSA}-$L_{I\text{-}RSA}$) and the ratio of amplitudes (estimated as $A_{RSA}/A_{I\text{-}RSA} - 1$) between MLR signals obtained by the RSA and I-RSA methods. Statistically significant differences between the two methods are expressed with asterisks (*: p-value < 0.05; **: p-value < 0.01).

Stimulation rate	L_{N_a}	L_{P_a}	L_{N_b}	L_{P_b}	$A_{N_a-P_a}$	$A_{N_b-P_b}$
8 Hz	0.00 (0.06)	−0.04 (0.07)	0.45 (1.31)	−0.05 (0.14)	0.00 (0.00)	0.00 (0.00)
20 Hz	−0.08 (0.21)	−0.03 (0.10)	0.11 (0.22)	−0.19 (0.26)	0.05 (0.05)	0.41 (0.26)*
40 Hz	−0.24 (0.64)	0.09 (0.22)	0.65 (1.44)	0.06 (0.44)	0.36 (0.10)**	0.48 (0.21)**
67 Hz	0.16 (0.31)	−0.30 (0.43)	−0.30 (0.76)	−1.31 (1.59)	−0.21 (0.06)**	−0.27 (0.10)**
100 Hz	0.13 (0.24)	0.07 (0.42)	−0.76 (1.18)	−2.44 (2.72)*	−0.27 (0.06)**	−0.33 (0.05)**
125 Hz	−0.03 (0.22)	−0.05 (0.50)	−0.37 (0.92)	−0.41 (1.22)	−0.23 (0.11)**	−0.27 (0.08)**

method, this analysis has shown that this method performs a highly accurate estimate of the template in both ABR and MLR signals at all rates and under all jittering conditions, which indicates that the I-RSA method is barely affected by interference associated with overlapping responses when the jitter is greater than, equal to, or shorter than the dominant period of the ABR/MLR components. Analysis of real ABR/MLR signals was consistent with the computer-simulated study: (a) No significant differences between ABR and MLR signals obtained by the RSA and I-RSA methods were observed when the jitter of the stimulation sequence was at least equal to the dominant period of the ABR/MLR signals; and (b) when this premise was not fulfilled, the AEP obtained by RSA was contaminated by interference due to overlapping adjacent responses.

The morphology of the recorded signals in the second experiment and the results of the analysis of latencies and amplitudes indicate that I-RSA allows accurate AEPs to be recorded using randomized stimulation sequences with jitter distributions both greater and lower than the dominant period of the ABR/MLR components. Furthermore, this experiment has revealed the limitations of the RSA method when the jitter of the stimulation sequences is shorter than the dominant period of the ABR/MLR components. This study also included an analysis of the differences between the estimation of latencies and ratio of amplitudes as carried out by the I-RSA and RSA methods. The results of this study were in accordance with the results obtained in the first experiment. These results showed that (a) estimates of real ABR signals by the I-RSA and RSA methods were very similar, suggesting that RSA can be used efficiently in applications that allow the use of a jitter higher than the dominant period of the ABR/MLR components, and (b) estimates of real MLR signals by the two methods presented significant differences owing to the low jitter relative to the dominant period of the MLR components in RSA, which did not allow the reduction by averaging of the interference associated with overlapping responses.

In conclusion, the results of this study indicate that the RSA method can be efficiently used for recording AEPs provided that the amount of jitter of the randomized stimulation sequence is greater than the dominant period of the ABR/MLR components. When this premise is not fulfilled, positive and negative components of the interference associated with overlapping responses cannot be canceled out in the averaging process, and the resulting AEP will not be reliable. The limitation of a minimum amount of jitter in RSA is not a significant constraint in the recording of ABR signals. In ABRs, the jitter must be greater than 2 ms in order for the response to be estimated accurately by the RSA method. Theoretically, this amount of jitter would allow the generation of stimulation sequences to record ABRs at rates of up to 1000 Hz (using randomized stimulation sequences ISI_{0-2}). However, the longer dominant period of the components of MLR signals entails the use of a minimum jitter of 25 ms, which constrains the use of the RSA method to rates of up to 80 Hz (using randomized stimulation sequences ISI_{0-25}). This stimulation rate may prove to be insufficiently high in certain applications. Additionally, the use of such high-jittered distributions may evoke auditory responses of different morphology, leading to inaccurate MLR signals, as invariance of the response over time would be wrongly assumed (Jewett *et al.*, 2004; Ozdamar and Bohorquez, 2006; Valderrama *et al.*, 2012, 2014a).

The I-RSA approach presented here would seem to be an efficient alternative to RSA when the amount of jitter used in the stimulation sequences is shorter than the dominant period of the ABR/MLR components. In this study, AEPs were successfully recorded by I-RSA at remarkably high stimulation rates: ABR signals were recorded at rates of up to 300 Hz and MLR signals were recorded for the first time with a method based on randomized stimulation at rates of up to 125 Hz. The performance of I-RSA maintains all the advantages of RSA: (a) It allows the jitter distribution to be controlled with precision, (b) stimulation sequences are easy to generate, and (c) it allows responses to be processed separately. Additionally, I-RSA is not constrained by the restriction of a minimum amount of jitter and convergence of this iterative procedure can be controlled with the correction factor. These advantages may prove to be of value in various research applications.

ACKNOWLEDGMENTS

This paper has been supported by research project TEC2009-14245, R&D National Plan (2008–2011), Ministry of Finance and Competition (Government of Spain); by research project GENIL-PYR 2014, Campus of International Excellence, Ministry of Finance and Competition (Government of Spain); and by Grant No. AP2009-3150 (FPU), Ministry of Education, Culture, and Sport (Government of Spain).

Bardy, F., Dillon, H., and Van Dun, B. (**2014a**). "Least-squares deconvolution of evoked potentials and sequence optimization for multiple stimuli under low-jitter conditions," Clin. Neurophysiol. **125**, 727–737.

Bardy, F., Van Dun, B., Dillon, H., and McMahon, C. M. (**2014b**). "Deconvolution of overlapping cortical auditory evoked potentials recorded using short stimulus onset-asynchrony ranges," Clin. Neurophysiol. **125**, 814–826.

Bekker, E. M., Overtoom, C. C. E., Kooij, J. J. S., Buitelaar, J. K., Verbaten, M. N., and Kenemans, J. L. (**2005**). "Disentangling deficits in adults with attention deficit/hyperactivity disorder," Arch. Gen. Psychiatry **62**, 1129–1136.

Bell, S. L., Allen, R., and Lutman, M. E. (**2001**). "The feasibility of maximum length sequences to reduce acquisition time of the middle latency response," J. Acoust. Soc. Am. **109**, 1073–1081.

Bell, S. L., Allen, R., and Lutman, M. E. (**2002**). "Optimizing the acquisition time of the middle latency response using maximum length sequences and chirps," J. Acoust. Soc. Am. **112**, 2065–2073.

Bohorquez, J., and Ozdamar, O. (**2006**). "Signal to noise ratio analysis of maximum length sequence deconvolution of overlapping evoked potentials," J. Acoust. Soc. Am. **119**, 2881–2888.

Bohorquez, J., and Ozdamar, O. (**2008**). "Generation of the 40-Hz auditory steady-state response (ASSR) explained using convolution," Clin. Neurophysiol. **119**, 2598–2607.

Bohorquez, J., Ozdamar, O., McNeer, R., and Morawski, K. (**2009**). "Clinical applications of evoked potential continuous loop averaging deconvolution (CLAD)," in *IFMBE Proceedings of the 25th Southern Biomedical Engineering Conference*, pp. 133–134.

Burkard, R., Shi, Y., and Hecox, K. E. (**1990**). "A comparison of maximum length and Legendre sequences for the derivation of brain-stem auditory-evoked responses at rapid rates of stimulation," J. Acoust. Soc. Am. **87**, 1656–1664.

Burkard, R. F., and Don, M. (**2007**). "The auditory brainstem response," in *Auditory Evoked Potentials: Basic Principles and Clinical Application*, edited by R. Burkard, M. Don, and J. Eggermont (Lippincott Williams & Wilkins, Baltimore, MD), pp. 229–253.

Bush, M. L., Jones, R. O., and Shinn, J. B. (**2008**). "Auditory brainstem response threshold differences in patients with vestibular schwannoma: A new diagnostic index," Ear, Nose Throat J. **87**, 458–462.

de Boer, J., Brennan, S., Lineton, B., Stevens, J., and Thornton, A. R. D. (**2007**). "Click-evoked otoacoustic emissions (CEOAEs) recorded from neonates under 13 hours old using conventional and maximum length sequence (MLS) stimulation," Hear. Res. **233**, 86–96.

Delgado, R. E., and Ozdamar, O. (**1994**). "Automated auditory brainstem response interpretation," IEEE Eng. Med. Biol. Mag. **13**, 227–237.

Delgado, R. E., and Ozdamar, O. (**2004**). "Deconvolution of evoked responses obtained at high stimulus rates," J. Acoust. Soc. Am. **115**, 1242–1251.

Don, M., Allen, A., and Starr, A. (**1977**). "Effect of click rate on the latency of auditory brain stem responses in humans," Ann. Otol., Rhinol., Laryngol. **86**, 186–195.

Eggermont, J. J. (**2007**). "Electric and magnetic fields of synchronous neural activity: Peripheral and central origins of AEPs," in *Auditory Evoked Potentials: Basic Principles and Clinical Application*, edited by R. Burkard, M. Don, and J. Eggermont (Lippincott Williams & Wilkins, Baltimore, MD), pp. 2–21.

Elberling, C., and Don, M. (**2007**). "Detecting and assessing synchronous neural activity in the temporal domain (SNR, Response detection)," in *Auditory Evoked Potentials: Basic Principles and Clinical Application*, edited by R. Burkard, M. Don, and J. Eggermont (Lippincott Williams & Wilkins, Baltimore, MD), pp. 102–123.

Eysholdt, U., and Schreiner, C. (**1982**). "Maximum length sequences: A fast method for measuring brain-stem-evoked responses," Audiology **21**, 242–250.

Fifer, R. C., and Sierra-Irizarry, B. (**1988**). "Clinical applications of the auditory middle latency response," Am. J. Otology **9**, 47–56.

Galambos, R., Makeig, S., and Talmachoff, P. J. (**1981**). "A 40-Hz auditory potential recorded from the human scalp," in Proc. Natl. Acad. Sci. U.S.A. **78**, 2643–2647.

Gutschalk, A., Oldermann, K., and Rupp, A. (**2009**). "Rate perception and the auditory 40-Hz steady-state fields evoked by two-tone sequences," Hear. Res. **257**, 83–92.

Hall, J. W. (**2007**). *New Handbook of Auditory Evoked Responses*, 1st ed. (Allyn and Bacon, Boston, MA), p. 750.

Hine, J. E., Ho, C.-T., Slaven, A., and Thornton, A. R. D. (**2001**). "Comparison of transient evoked otoacoustic emission thresholds recorded conventionally and using maximum length sequences," Hear. Res. **156**, 104–114.

Jewett, D. L., Caplovitz, G., Baird, B., Trumpis, M., Olson, M. P., and Larson-Prior, L. J. (**2004**). "The use of QSD (q-sequence deconvolution) to recover superposed, transient evoked-responses," Clin. Neurophysiol. **115**, 2754–2775.

Jewett, D. L., and Williston, J. S. (**1971**). "Auditory-evoked far fields averaged from the scalp of humans," Brain **94**, 681–696.

Jiang, Z. D., Brosi, D. M., Shao, X. M., and Wilkinson, A. R. (**2000**). "Maximum Length Sequence brainstem auditory evoked responses in term neonates who have perinatal hypoxiaischemia," Pediatr. Res. **48**, 639–645.

Jiang, Z. D., Wu, Y. Y., and Wilkinson, A. R. (**2009**). "Age-related changes in BAER at different click rates from neonates to adults," Acta Paediatr. **98**, 1284–1287.

Kacker, S. K., and Deka, R. C. (**1986**). "Auditory brainstem evoked responses in Meniere's disease," Indian J. Otolaryngol. **38**, 14–17.

Kjaer, M. (**1980**). "Brain stem auditory and visual evoked potentials in multiple sclerosis," Acta Neurol. Scan. **62**, 14–19.

Lasky, R. E. (**1984**). "A developmental study on the effect of stimulus rate on the auditory evoked brain-stem response," Electroencephalogr. Clin. Neurophysiol. **59**, 411–419.

Lasky, R. E. (**1997**). "Rate and adaptation effects on the auditory evoked brainstem response in human newborns and adults," Hear. Res. **111**, 165–176.

Lavoie, B. A., Barks, A., and Thornton, A. R. D. (**2010**). "Linear and nonlinear temporal interaction components of mid-latency auditory evoked potentials obtained with maximum length sequence stimulation," Exp. Brain Res. **202**, 231–237.

Leung, S., Slaven, A., Thornton, A. R. D., and Brickley, G. J. (**1998**). "The use of high stimulus rate auditory brainstem responses in the estimation of hearing threshold," Hear. Res. **123**, 201–205.

Lina-Granade, G., Collet, L., Morgon, A., and Salle, B. (**1993**). "Maturation and effect of stimulus rate on brainstem auditory evoked potentials," Brain and Development **15**, 263–269.

Oppenheim, A. V., and Schafer, R. W. (**1999**). *Discrete-Time Signal Processing*, 2nd ed. (Prentice-Hall, Upper Saddle River, NJ), p. 870.

Ozdamar, O., and Bohorquez, J. (**2006**). "Signal-to-noise ratio and frequency analysis of continuous loop averaging deconvolution (CLAD) of overlapping evoked potentials," J. Acoust. Soc. Am. **119**, 429–438.

Ozdamar, O., Bohorquez, J., and Ray, S. S. (**2007**). "$P_b(P_1)$ resonance at 40 Hz: Effects of high stimulus rate on auditory middle latency responses (MLRs) explored using deconvolution," Clin. Neurophysiol. **118**, 1261–1273.

Ozdamar, O., Delgado, R. E., Yavuz, E., Thombre, K., and Acikgoz, N. (**2003b**). "Deconvolution of auditory evoked potentials obtained at high stimulus rates," in *Proceedings of the 1st International IEEE EMBS Conference on Neural Engineering*, pp. 285–288.

Ozdamar, O., Delgado, R. E., Yavuz, E., Thombre, K., and Anderson, M. (**2003a**). "Acquisition of ABRs at very high stimulation rate using CLAD (Continuous Loop Algorithm Deconvolution)," ARO Vol. 26, abstract number 173.

Pastor, M. A., Artieda, J., Arbizu, J., Marti-Climent, J. M., Penuelas, I., and Masdeu, J. C. (**2002**). "Activation of human cerebral and cerebellar cortex by auditory stimulation at 40 Hz," J. Neurosci. **22**, 10501–10506.

Picton, T. W., Champagne, S. C., and Kellet, A. J. C. (**1992**). "Human auditory evoked potentials recorded using maximum length sequences," Electroencephalogr. Clin. Neurophysiol. **84**, 90–100.

Podoshin, L., Ben-David, Y., Pratt, H., Fradis, M., and Feiglin, H. (**1986**). "Noninvasive recordings of cochlear evoked potentials in Meniere's disease," Arch. Otolaryngol., Head Neck Surg. **112**, 827–829.

Pratt, H. (**2007**). "Middle-latency responses," in *Auditory Evoked Potentials: Basic Principles and Clinical Application*, edited by R. Burkard, M. Don, and J. Eggermont (Lippincott Williams & Wilkins, Baltimore, MD), pp. 463–481.

Pratt, H. (**2011**). "Sensory ERP components," in *Oxford Handbook of Event-Related Potential Components*, edited by E. S. Kappenman and S. J. Luck (Oxford University Press, New York), pp. 1–35.

Pratt, H., and Sohmer, H. (**1976**). "Intensity and rate functions of cochlear and brainstem evoked responses to click stimuli in man," Arch. Oto-Rhino-Laryngol. **212**, 85–92.

Presacco, A., Bohorquez, J., Yavuz, E., and Ozdamar, O. (**2010**). "Auditory steady-state responses to 40 Hz click trains: Relationship to middle latency, gamma band and beta band responses studied with deconvolution," Clin. Neurophysiol. **121**, 1540–1550.

Rudell, A. (**1987**). "A fiber tract model of auditory brain-stem responses," Electroencephalogr. Clin. Neurophysiol. **67**, 53–62.

Stockard, J. J., Stockard, J. E., and Sharbrough, F. W. (**1978**). "Nonpathologic factors influencing brainstem auditory evoked potentials," Am. J. EEG Technol. **18**, 177–209.

Stone, J. L., Calderon-Arnulphi, M., Watson, K. S., Patel, K., Mander, N. S., Suss, N., Fino, J., and Hughes, J. R. (**2009**). "Brainstem auditory evoked potentials—A review and modified studies in healthy subjects," J. Clin. Neurophysiol. **26**, 167–175.

Talsma, D., and Woldorff, M. G. (**2005**). "Methods for estimating and removal of artifacts and overlap in ERP waveforms," in *Event-Related Potentials: A Methods Handbook*, edited by T. H. Handy (MIT Press, Cambridge, MA), pp. 115–148.

Thornton, A. R. D. (**2007**). "Instrumentation and recording parameters," in *Auditory Evoked Potentials: Basic Principles and Clinical Application*, edited by R. Burkard, M. Don, and J. Eggermont (Lippincott Williams & Wilkins, Baltimore, MD), pp. 73–101.

Thornton, A. R. D., Lineton, B., Baker, V. J., and Slaven, A. (**2006**). "Nonlinear properties of otoacoustic emissions in normal and impaired hearing," Hear. Res. **219**, 56–65.

Thornton, A. R. D., and Slaven, A. (**1993**). "Auditory brainstem responses recorded at fast stimulation rates using maximum length sequences," Br. J. Audiol. **27**, 205–210.

Tuliani, J. (**2001**). "De Bruijn sequences with efficient decoding algorithms," Discrete Math. **226**, 313–336.

Valderrama, J. T., Alvarez, I., de la Torre, A., Segura, J. C., Sainz, M., and Vargas, J. L. (**2011**). "Educational approach of a BAER recording system based on experiential learning," Tech. Technol. Ed. Manage. **6**, 876–889.

Valderrama, J. T., Alvarez, I., de la Torre, A., Segura, J. C., Sainz, M., and Vargas, J. L. (**2012**). "Recording of auditory brainstem response at high stimulation rates using randomized stimulation and averaging," J. Acoust. Soc. Am. **132**, 3856–3865.

Valderrama, J. T., de la Torre, A., Alvarez, I., Segura, J. C., Sainz, M., and Vargas, J. L. (**2014c**). "A flexible and inexpensive high-performance auditory evoked response recording system appropriate for research purposes," Biomed. Tech. **59**(5), 447–459.

Valderrama, J. T., de la Torre, A., Alvarez, I., Segura, J. C., Thornton, A. R. D., Sainz, M., and Vargas, J. L. (**2013**). "Auditory middle latency responses recorded at high stimulation rates using randomized stimulation and averaging," in *International Evoked Response Audiometry Study Group (IERASG) Meeting*, New Orleans, LA, June 9–13, pp. 56.

Valderrama, J. T., de la Torre, A., Alvarez, I., Segura, J. C., Thornton, A. R. D., Sainz, M., and Vargas, J. L. (**2014a**). "A study of adaptation mechanisms based on ABR recorded at high stimulation rate," Clin. Neurophysiol. **125**, 805–813.

Valderrama, J. T., de la Torre, A., Alvarez, I., Segura, J. C., Thornton, A. R. D., Sainz, M., and Vargas, J. L. (**2014b**). "Automatic quality assessment and peak identification of auditory brainstem responses with fitted parametric peaks," Comput. Methods Programs Biomed. **114**, 262–275.

Wang, T., Huang, J.-H., Lin, L., and Zhan, C. A. (**2013**). "Continuous- and discrete-time stimulus sequences for high stimulus rate paradigm in evoked potential studies," Comput. Math. Methods Med. **2013**, 396034.

Wang, A., Moraux, A., Liang, M., and Iannetti, G. (**2008**). "The enhancement of the N1 wave elicited by sensory stimuli presented at very short inter-stimulus intervals is a general feature across sensory systems," PLoS One **3**, e3929.

Wang, T., Ozdamar, O., Bohorquez, J., Shen, Q., and Cheour, M. (**2006**). "Wiener filter deconvolution of overlapping evoked potentials," J. Neurosc. Methods **158**, 260–270.

Woldorff, M. G. (**1993**). "Distortion of ERP averages due to overlap from temporally adjacent ERPs: Analysis and correction," Psychophysiology **30**, 98–119.

Wong, P. K. H., and Bickford, R. G. (**1980**). "Brain stem auditory evoked potentials: the use of noise estimate," Electroencephalogr. Clin. Neurophysiol. **50**, 25–34.

Yagi, T., and Kaga, K. (**1979**). "The effect of the click repetition rate on the latency of the auditory evoked brain stem response and its clinical use for a neurological diagnosis," Arch. Oto-Rhino-Laryngol. **222**, 91–96.

Zollner, C., Karnahl, T., and Stange, G. (**1976**). "Input-output function and adaptation behaviors of the five early potentials registered with the earlobe-vertex pick up," Arch. Oto-Rhino-Laryngol. **212**, 23–33.